Mon. Not. R. Astron. Soc. **000**, **??–??** (20??)   Printed 12 January 2013   (MN LaTeX style file v2.2)

The Halo Occupation Distribution of Black Holes: Dependence on Mass

Colin Degraf[1], Matthew Oborski[1], Tiziana Di Matteo[1], Suchetana Chatterjee[2], Daisuke Nagai[2,3], Zheng Zheng[3], Jonathan Richardson[2]
[1] *McWilliams Center for Cosmology, Carnegie Mellon University, 5000 Forbes Avenue, Pittsburgh, PA 15213, USA*
[2] *Department of Astronomy, Yale University, New Haven, CT 06520 USA*
[3] *Department of Physics, Yale University, New Haven, CT 06520 USA*

arXiv:1102.1437v1 [astro-ph.CO] 7 Feb 2011

Accepted 20?? ???? ??. Received 20?? ???? ??; in original form 20?? xx

ABSTRACT

We investigate the halo occupation distribution (HOD) of black holes within a hydrodynamic cosmological simulation that directly follows black hole growth. Similar to the HOD of galaxies/subhalos, we find that the black hole occupation number can be described by the form $N_{\rm BH} \propto 1 + (M_{\rm Host})^{\alpha}$ where α evolves mildly with redshift indicating that a given mass halo ($M_{\rm Host}$) at low redshift tends to host fewer BHs than at high redshift (as expected as a result of galaxy and BH mergers). We further divide the occupation number into contributions from black holes residing in central and satellite galaxies within a halo. The distribution of $M_{\rm BH}$ within halos tends to consist of a single massive BH (distributed about a peak mass strongly correlated with $M_{\rm Host}$), and a collection of relatively low-mass secondary BHs, with weaker correlation with $M_{\rm Host}$. We also examine the spatial distribution of BHs within their host halos, and find they typically follow a power-law radial distribution (i.e. much more centrally concentrated than the subhalo distribution). Finally, we characterize the host mass for which BH growth is feedback dominated (e.g. star formation quenched). We show that halos with $M_{\rm Host} > 3 \times 10^{12} M_{\odot}$ have primary BHs that are feedback dominated by $z \sim 3$ with lower mass halos becoming increasingly more affected at lower redshift.

1 INTRODUCTION

Supermassive black holes have been found to be at the center of most galaxies (Kormendy & Richstone 1995), and the correlation between these central black holes and their host galaxy properties have been extensively studied (see, e.g. Magorrian et al. 1998; Ferrarese & Merritt 2000; Gebhardt et al. 2000; Tremaine et al. 2002; Graham & Driver 2007). Gas accretion onto supermassive black holes leads to AGN and quasar activity, producing bright objects idea for observations. One of the primary means of observationally studying quasars is by looking at their clustering properties, including redshift evolution (e.g. La Franca et al. 1998; Porciani et al. 2004; Croom et al. 2005; Shen et al. 2007; Myers et al. 2007a; da Ângela et al. 2008; Shen et al. 2009; Ross et al. 2009) and luminosity dependence (see, e.g., Croom et al. 2005; Myers et al. 2007a; da Ângela et al. 2008; Shen et al. 2009). By looking at the clustering strength of different quasar populations, one can estimate the mass of the typical host halo (Lidz et al. 2006; Ross et al. 2009; Bonoli et al. 2009; Shen et al. 2009), thereby getting a sense of how black holes populate halos. This information can then be used to infer details about several properties, such as quasar lifetimes (Haiman & Hui 2001; Martini & Weinberg 2001), which can be constrained by comparing the observed quasar number density to the predicted density of the halo mass-function prediction using the typical host halos.

Recently, quasar clustering studies have found evidence for a bias in the small-scale correlation function (Hennawi et al. 2006; Myers et al. 2007b, 2008), and DeGraf et al. (2010b) used cosmological hydrodynamic simulations to investigate BH clustering, finding that the existence of multiple BHs within individual galaxies has a significant effect on the small-scale correlation function which could explain this observed small-scale excess. However, this was an indirect means of exploring the relation between BHs and their typical host halos, and a more direct investigation is necessary to fully understand how BHs populate halos.

With the aid of simulations, the opposite approach can be taken for such a direct investigation: instead of using clustering to predict the halos occupied by BHs, the DM halos can be directly probed to get BH occupation properties, which can then be extended to explore clustering properties. This technique has been used extensively for galaxies in the form of the Halo Occupation Distribution (HOD) (see, e.g. Berlind & Weinberg 2002; Kravtsov et al. 2004; Zheng et al. 2005). At the most basic level, an HOD model characterizes the number of objects within halos as a function of the halo mass, and how they are spatially distributed within the

© 20?? RAS

halo. Given these simple statistical distributions, the HOD model can be used to populate halos in N-body simulations (e.g. Benson et al. 2000; Berlind et al. 2003; Brown et al. 2008) and, assuming the occupation distribution is independent of the large scale environment (Lemson & Kauffmann 1999; Berlind et al. 2003), can be used to analytically calculate the clustering statistics for a given cosmological model (see, e.g. Seljak 2000; Berlind & Weinberg 2002). The galaxy HOD model can then be extended further by looking at how the occupation properties depend upon various galaxy parameters, such as galaxy luminosity, color, or morphology, which can be used to better understand the physics of galaxy formation and evolution (e.g. Yoshikawa et al. 2001; Berlind et al. 2003; Zehavi et al. 2005; Zheng et al. 2007; Reid & Spergel 2009; Zehavi et al. 2010).

Despite its overall success for galaxies, the HOD technique has not been applied to black holes. In this paper we extend the work done in DeGraf et al. (2010b) by directly investigating how BHs populate dark matter halos using the HOD formalism. In addition to characterizing the occupation number of BHs in DM halos, we investigate the distribution of BH masses within the halo, as well as their spatial distribution among the component subhalos. Additionally, in an upcoming paper (Chatterjee et al., in prep) we will further extend this model to incorporate the luminosity dependencies of the black holes. By providing these details of a BH HOD model from a hydrodynamic simulation, we hope to improve the techniques available for both semi-analytic BH models, and theoretical studies of BH clustering.

In Section 2 we describe the simulation used, with particular emphasis on how the black holes are modeled. In Section 3 we investigate the BH occupation number both for halos and for central and satellite galaxies (3.1), the distribution of BH masses as a function of host halo mass (3.2), and the spatial distribution of the BHs within their parent halos (3.3). Finally, in section (3.4) we look at when the feedback from the BH begins to suppress further BH growth, and we summarize our results in Section 4.

2 METHOD

2.1 Numerical simulation

In this study, we analyse the set of simulations published in Di Matteo et al. (2008). Here we present a brief summary of the simulation code and the method used. We refer the reader to Di Matteo et al. (2008) for all details.

The code we use is the massively parallel cosmological TreePM–SPH code Gadget2 (Springel 2005), with the addition of a multi–phase modeling of the ISM, which allows treatment of star formation (Springel & Hernquist 2003), and black hole accretion and associated feedback processes (Springel et al. 2005; Di Matteo et al. 2005). Detailed studies of the prescription for accretion and associated feedback from massive black holes and associated predictions have been presented in Sijacki et al. (2007); Di Matteo et al. (2008); Colberg & di Matteo (2008); Croft et al. (2009); DeGraf et al. (2010a). Important for our discussion is that the model has been shown to reproduce remarkably well both the observed $M_{\rm BH}-\sigma$ relation and total black hole mass density $\rho_{\rm BH}$ (Di Matteo et al. 2008), as well as the quasar luminosity functions and its evolution in optical, soft and hard X-ray band (DeGraf et al. 2010a). Thus the model, within its intrinsic limitations, appears to serve as a fair standard for representing growth, activity, and evolution of massive black holes in numerical simulations, at least within the context of cosmological growth of black holes and not the detailed accretion physics (the detailed treatment of which is completely infeasible in cosmological simulations). We note also that at least two independent teams (Booth & Schaye 2009; Johansson et al. 2008) now have also adopted the same modeling for black hole accretion, feedback and BH mergers in the context of hydrodynamic simulations. These independent works, in particular the cosmological simulations by Booth & Schaye (2009) (part of the OWLS program) have fully and independently explored the parameter space of the reference model of Di Matteo et al. (2008), as well as variations to some prescriptions. This large body of already existing work and investigations make this particular model somewhat of a good choice for further study.

Within the simulation, black holes are simulated with collisionless particles that are created in newly emerging and resolved groups/galaxies. To find these groups, a friends–of–friends group finder is called at regular intervals on the fly (in time intervals equally spaced in $\log_{10}(a)$, with $\Delta \log a = \log 1.25$), finding groups based on particle separations below a specified cutoff. Each group with a mass above $5 \times 10^{10} h^{-1}\,{\rm M}_\odot$ that does not already contain a black hole is provided with one by converting its densest particle into a sink particle with a seed mass of $M_{\rm BH,seed} = 5 \times 10^5 h^{-1}\,{\rm M}_\odot$. This seeding prescription was selected to reasonably match the expected formation of supermassive black holes either by collapse of a supermassive star to a BH with $M_{\rm BH} \sim M_{\rm seed}$ (e.g. Bromm & Loeb 2003; Begelman et al. 2006) or by Pop III stars collapsing into $\sim 10^2 M_\odot$ BHs at $z \sim 30$ followed by exponential growth (Bromm & Larson 2004; Yoshida et al. 2006), reaching $\sim M_{\rm seed}$ by the time the group reaches $\sim 10^{10} M_\odot$. After insertion, the black hole particle grows in mass via both accretion of surrounding gas and by merging with other black holes. The gas accretion is modeled according to $\dot{M}_{\rm BH} = \frac{4\pi G^2 M_{\rm BH}^2 \rho}{(c_s^2+v^2)^{3/2}}$ (Hoyle & Lyttleton 1939; Bondi & Hoyle 1944; Bondi 1952), where ρ is the local gas density, c_s is the local sound speed, and v is the velocity of the BH relative to the surrounding gas. Note that to allow for the initial rapid BH growth necessary to produce supermassive BHs of $\sim 10^9 M_\odot$ at early time ($z \sim 6$), we allow for mildly super-Eddington accretion (consistent with models of, e.g., Volonteri & Rees 2006; Begelman et al. 2006), but limit super-Eddington accreion to a maximum of $3 \times \dot{M}_{\rm Edd}$ to prevent artificially high values.

The accretion rate of each black hole is used to compute the bolometric luminosity, $L = \eta \dot{M}_{\rm BH} c^2$ (Shakura & Sunyaev 1973). Here η is the radiative efficiency, and it is fixed at 0.1 throughout the simulation and this analysis. Some coupling between the liberated luminosity and the surrounding gas is expected, modeled in the simulation by isotropically depositing the 5 per cent of the luminosity as thermal energy to the local black hole kernal. This parameter is fixed at 5 per cent based on earlier galaxy merger simulations such that the normalization of the $M_{\rm BH} - \sigma$ relation is reproduced (Di Matteo et al. 2005).

The other means of black hole growth is via mergers. When dark matter halos merge into a single halo, the

Table 1. Numerical Parameters

Boxsize h^{-1}Mpc	N_p	$m_{\rm DM}$ $h^{-1}M_\odot$	$m_{\rm gas}$ $h^{-1}M_\odot$	ϵ h^{-1}kpc
33.75	2×486^3	2.75×10^7	4.24×10^6	2.73

N_p: Total number of particles
$m_{\rm DM}$: Mass of dark matter particles
$m_{\rm gas}$: Initial mass of gas particles
ϵ: Comoving gravitational softening length

black holes typically fall toward the center of the new halo, eventually merging with one another. For these cosmological volumes, it is not possible to directly calculate the details of the infalling BHs at the smallest scales, so a subresolution merger prescription is used. Since the merging BHs are typically found in a gaseous environment at the center of a galaxy, we assume that the final coalescence will be rapid (Makino & Funato 2004; Escala et al. 2004; Mayer et al. 2007). Thus our BHs merge when they come within the spatial resolution of the simulation. However, to prevent merging of BHs which are rapidly passing one another, mergers are permitted only if the velocity of the BHs relative to one another is small (comparable to the local sound speed).

In addition to having been used in galaxy merger simulations to investigate the regulation of BH growth and correlation with host galaxies (Di Matteo et al. 2005; Robertson et al. 2006; Hopkins et al. 2007a), Di Matteo et al. (2008) previously investigated the validity of this method of modeling black holes in these cosmological simulations, finding that in addition to producing an $M_{\rm BH}-\sigma$ relation that matches observations, the black hole mass density matches values inferred from the integrated x-ray luminosity function (Shankar et al. 2004; Marconi et al. 2004) and the accretion rate density is consistent with the constraints of Hopkins et al. (2007b).

2.2 Simulation parameters

The simulation analysed in this paper populates 2×486^3 particles in a moderate volume of side length $33.75h^{-1}$Mpc (See Table 1 for additional simulation parameters). This moderate boxsize prevents the simulation from being run below $z\sim1$ to keep the fundamental mode linear, but provides a large enough scale to produce statistically significant quasar populations. The limitation on the boxsize is necessary to allow for appropriate resolution to carry out the subgrid physics in a converged regime (for further details on the simulation methods, parameters and convergence studies see Di Matteo et al. (2008)).

2.3 Subgroup finder algorithm

In addition to the on-the-fly friends-of-friends algorithm used to identify groups, a modified version of the SUBFIND algorithm (Springel et al. 2001) was run on the FoF-identified groups to determine the component subgroups (*i.e.* galaxies) within each group. These subgroups are defined as locally overdense, self-bound particle groups. To identify these regions, the algorithm analyzes each particle within the parent group in order of decreasing density. For each particle i, the density of the 32 nearest neighbors are checked. If none are denser than particle i, it forms the basis for a new subgroup. If a single particle denser than i is found, or if the closest two denser particles belong to the same subgroup, particle i is assumed to be a member of that subgroup. If the two nearest particles denser than i are members of different subgroups, these two subgroups are stored as subgroup candidates, and are then joined into a new subgroup also containing i. After checking each particle in this manner, particles are checked for gravitational binding within their parent subgroup based on their position relative to the position of the most bound particle and the velocity relative to the mean velocity of particles in the group. Any particle with positive total energy is considered unbound, and is removed from the subgroup, leaving the group divided up into its component subgroups (galaxies).

3 RESULTS

3.1 Black Hole Occupation Number

The most basic component of the HOD model is the occupation number. In Figure 1 we show the mean occupation number for both BHs (solid black line) and subgroups (dashed black line) as a function of host halo mass, as well as the the exact number of BHs found in each individual group (green dots). Note that these numbers are based on the full BH population with no mass cut; see Section 3.2 for the BH mass distribution. We also show the contributions to $\langle N_{\rm BH}\rangle$ arising from BHs found in the central (i.e. most massive) galaxy (red line) and those found in satellite galaxies (blue line). We note that this is fundamentally different from the traditional galaxy HOD model, in which 'central' galaxy is of course just one. Multiple black holes can be found in a central galaxy (at least at low redshift as remnants of previous mergers) and therefore we do not have this restriction. For clarity, a schematic representation of these components (and some further subdivision we will discuss below) is shown in Figure 2.

In analogy with standard HOD models for the galaxy population we model the total, central and satellite BH occupation number (where $\langle N_{\rm BH,tot}\rangle = \langle N_{\rm BH,cen}\rangle + \langle N_{\rm BH,sat}\rangle$) as:

$$\langle N_{\rm BH,tot}\rangle = 1 + \left(\frac{M_{\rm Host}}{M_0}\right)^{\alpha_{\rm tot}}, \tag{1}$$

$$\langle N_{\rm BH,cen}\rangle = 1 + \left(\frac{M_{\rm Host}}{M_1}\right)^{\alpha_{\rm cen}}, \tag{2}$$

$$\langle N_{\rm BH,sat}\rangle = \left(\frac{M_{\rm Host}}{M_2}\right)^{\alpha_{\rm sat}} \tag{3}$$

respectively. where $M_{\rm Host}$ is the halo mass of the host, M_0, M_1 and M_2 are normalization constants which represent the host masses for which we have a total of typically two black holes per host, two black holes in the central galaxy and one in a satellite galaxy, respectively. Finally $\alpha_{\rm tot}, \alpha_{\rm cen}$ and $\alpha_{\rm sat}$ are the exponents of the power law functions above. Note that Equations 1-3 are not self consistent, but rather Equations 2-3 provide an alternative parameterization from Equation 1.

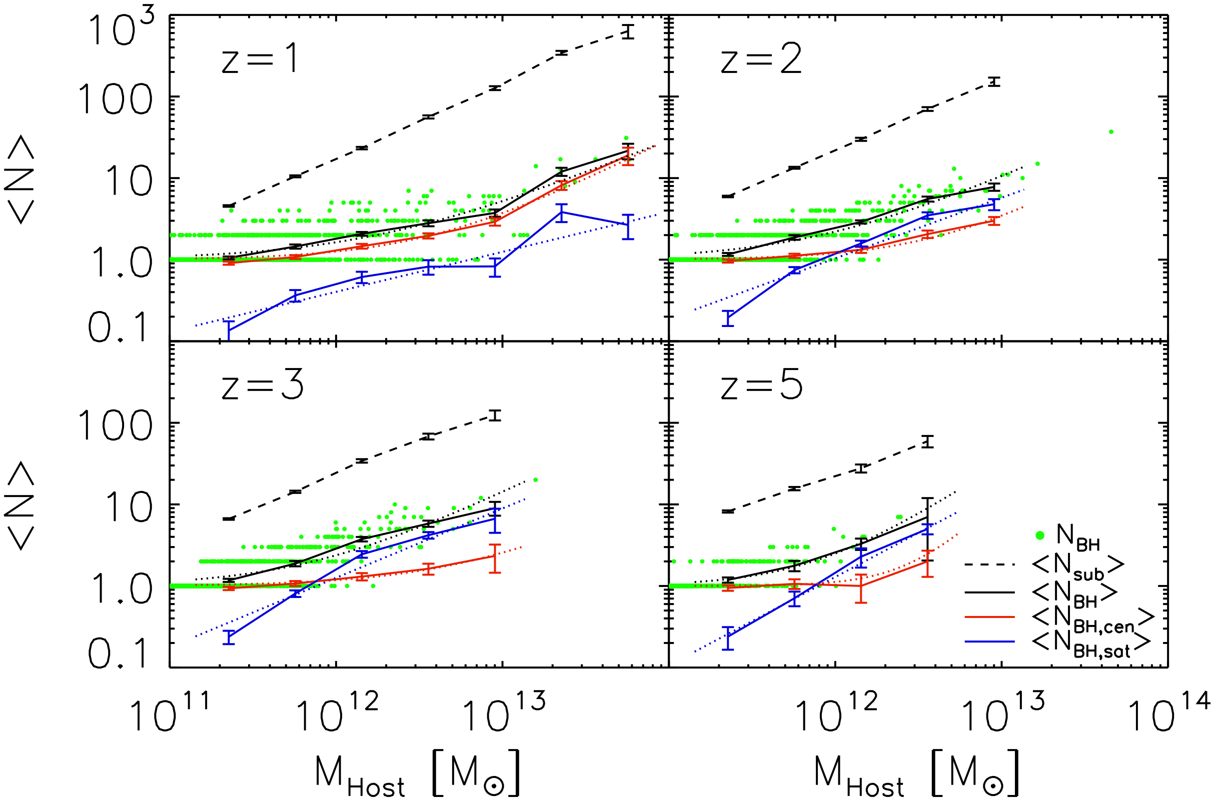

Figure 1. Mean occupation number of subhalos (dashed black line), total black holes (solid black line), black holes in the central galaxy (red), and black holes in the satellite galaxies (blue). We also show the number of BHs in each individual group (green dots), and the fits to the BH occupation number using Eqns. 1-3 and Table 2 (dotted lines).

Standard galaxy HOD usually have a form $\langle N_{\rm gal,tot}\rangle = \langle N_{\rm gal,cen}\rangle + \langle N_{\rm gal,sat}\rangle$, here for BHs $\langle N_{\rm gal,cen}\rangle$ has been replaced with a constant (equal to one) to represent our seeding condition (which artificially imposes this condition) and the power law forms $\langle N_{\rm gal,sat}\rangle$ is similar to the ones above. Note again, here we have introduced an additional power law for modelling the $N_{\rm BH,cen}$ which allow us to characterize the BH numbers in central galaxies.

Throughout this paper we refer to the most massive BH in a given group as the 'primary BH' while the remaining BHs are referred to as 'secondary BHs' (gained by merging with other BH-hosting halos; see Fig.2).

Note this makes $\langle N_{\rm BH,secondary}\rangle = \left(\frac{M_{\rm Host}}{M_0}\right)^{\alpha_{\rm tot}}$ by definition (given Equation 1). This formulation is advantageous as it can be used in clustering calculations in the same manner as the general galaxy HOD (see, e.g. Berlind & Weinberg 2002; Kravtsov et al. 2004; Zheng 2004).

The function for $\langle N_{\rm BH,cen}\rangle$ also includes a constant (equal to one) since BHs are seeded in the central subgroup. The form of $\langle N_{\rm BH,sat}\rangle$ lacks this constant since we do not seed subgroups with BHs, and thus there need not be any BHs found in the satellite galaxies. We examine each $\langle N\rangle$ to its appropriate form (Eqn. 1-3) based on halos at least twice the threshold mass for seeding BHs (to avoid considering just-seeded halos). The results of these models are plotted on Figure 1 as dotted lines. We emphasize that these simple fits are intended to provide a framework within which to get the typical number of BHs (total, satellite, and central) for the mass ranges probed in our simulation, but care should be taken when extrapolating to higher masses, particularly at high redshift where we have few data points.

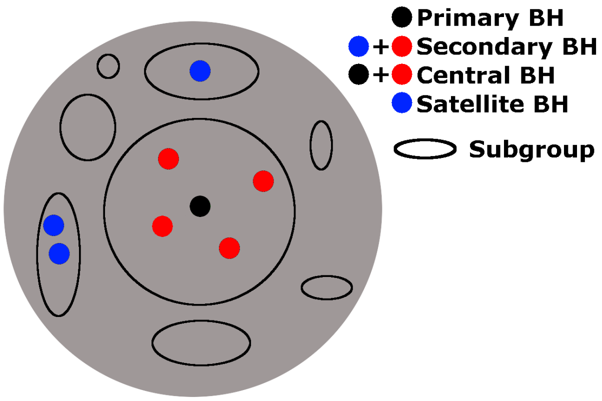

Figure 2. Cartoon representation of terminology used. The grey circle represents a single large halo, with subhalos shown as black ellipses. Primary BH: the most massive BH found in the halo (black). Central BH: All BHs found in the central (most massive) subhalo (red+black). Satellite BH: All BHs found in satellite subhalos (blue). Secondary BH: Any non-primary BH (blue+red).

We see that $\langle N_{\rm BH}\rangle$ exhibits a general trend of mildly decreasing slope (α) with decreasing redshift, and that halos at low redshift tend to have fewer BHs than halos with comparable mass at high redshift. To further understand this effect, in Figure 3 we show the ratio of $\langle N_{\rm BH,secondary}\rangle$

Table 2. Best fitting HOD parameters for Equations 1-3.

	Redshift			
	1	2	3	5
$\alpha_{\rm tot}$	0.82	0.90	0.98	1.3
M_0	1.7×10^{12}	8.1×10^{11}	7.2×10^{11}	7.3×10^{11}
$\alpha_{\rm cen}$	1.02	1.1	0.94	2.0
M_1	3.7×10^{12}	4.4×10^{12}	6.2×10^{12}	2.9×10^{12}
$\alpha_{\rm sat}$	0.49	0.74	0.85	1.1
M_2	6.4×10^{12}	9.5×10^{11}	7.6×10^{11}	7.9×10^{11}

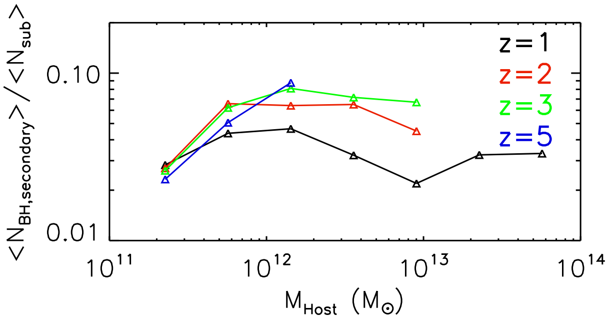

Figure 3. Ratio of $\langle N_{\rm BH,secondary}\rangle$ to $\langle N_{\rm subhalo}\rangle$ at z=1 (black), 2 (red), 3 (green), and 5 (blue).

to $\langle N_{\rm subhalos}\rangle$. We note that $\langle N_{\rm subhalos}\rangle$ is sensitive to the mass threshold used to define a subhalo. In this paper, we consider any subgroup found by the SUBFIND algorithm (see section 2.3) to be a subhalo. However, we note that although the normalization of $\langle N_{\rm subhalos}\rangle$ is sensitive to the mass threshold, the slope is not. To avoid delving into the issue of subgroup definitions and the model-dependencies therein, we limit ourselves to investigating how the ratio evolves, which does not exhibit significant dependence on the mass threshold. In low mass halos, the ratio does not evolve with redshift, and at each redshift there are fewer BHs per subhalo for the low-mass halos. This is expected since these are halos close to the threshold mass for seeding a BH, and few will have undergone a merger that can lead to a secondary BH. However, we note that more massive halos at low redshift tend to have fewer BHs per subhalo (and fewer BHs in general) than the corresponding halos at high redshift. This decrease is likely a result of changes in the halo and BH merger rates. Because the number of BHs in a halo depends both on the rate at which new BHs enter the halo (via halo mergers) and the rate at which BHs within the halo merge with each other, a decrease in the halo merger rate relative to the BH merger rate would explain the decreased number of BHs.

To characterize the scatter in $N_{\rm BH}$, in Figure 4 we plot the probability distribution $P(N_{\rm BH,secondary}|M)$ (the probability of a halo of mass M hosting $N_{\rm BH,secondary}$ BHs in addition to the initially-seeded, primary BH) for several ranges of host halo masses (filled circles with Poisson error bars). For comparison, we show a Poisson distribution with the same mean as the specified host mass range (dotted line). We see that the distribution of $N_{\rm BH,sat}$ is extremely close to the Poisson distribution for the lower mass ranges (where our simulation has a large sample of halos). Even for high mass halos, where our statistics are poor, it appears largely consistent with a Poisson distribution. We note that we have chosen to plot the probability distribution for the secondary BHs rather than the total number of BHs since the existence of the primary BH is a condition enforced by our simulation which distorts $P(N|M)$ away from a Poisson distribution (by removing the possibility of $N_{\rm BH} = 0$). However, this is an expected effect from the model for seeding BHs within our simulation, and we emphasize that the the physically-significant $N_{\rm BH,secondary}$ is well fit by a Poisson distribution about $\langle N_{\rm BH,secondary}\rangle$. We also note that although we have only plotted the distribution of $N_{\rm BH,secondary}$, we have also found that $N_{\rm BH,cen} - 1$ (to avoid inclusion of the model-imposed primary BH) and $N_{\rm BH,sat}$ both follow an approximate Poisson distribution as well.

3.2 Black Hole Conditional Mass Function

Another important facet of the model is the mass distribution of BHs populating halos. To investigate this we produce a conditional mass function (CMF), similar to the conditional luminosity function done for galaxies (see, e.g. Yang et al. 2003). For this, we use $\frac{dN_{\rm BH}}{d\log M_{\rm BH}}$, the mean number of BHs per logarithmic BH mass bin found in halos of mass $M_{\rm Host}$. We plot this quantity in Figure 5 for several host halo mass ranges at z=1,3. Here we see that in low mass halos, regardless of redshift, the BHs tend to be close to the seed mass, as expected. In higher mass halos, we find the distribution to be bimodal. The primary BH mass is distributed about a $M_{\rm Host}$-dependent peak, while the remaining BHs follow an approximate power law, with the majority of secondary BHs being near the seed mass. The secondary BH CMF is also mass-dependent, with the CMF in lower mass halos dropping faster with increasing $M_{\rm BH}$ than in lower mass halos. The secondary mass distribution always peaks at the seed mass, however, regardless of redshift or host halo mass.

The conditional mass function for the primary (i.e. most-massive) black hole can be approximated by a Gaussian distribution (in $\log_{10}(M_{\rm BH})$) with an integrated area of one

$$\frac{dN_{\rm BH,primary}}{d\log M_{\rm BH}} = \frac{1}{\sqrt{2\pi\sigma^2}} e^{-\frac{(\log_{10}(M_{\rm BH})-\mu)^2}{2\sigma^2}}. \tag{4}$$

The best fitting parameters for this function are provided in Table 3. Note there is only a single group above $10^{13} M_\odot$ at z=3, so no fitting parameters are given for that mass range. From these fits we can see that the typical primary BH mass grows roughly proportionally to the host mass range, and is approximately independent of redshift. Furthermore, the CMF for secondary BHs is reasonably well-fit by a simple power law

$$\frac{dN_{\rm BH,secondary}}{d\log M_{\rm BH}} = \left(\frac{M_{\rm BH}}{M_{0,\rm Host}}\right)^{\alpha}, \tag{5}$$

the parameters for which are given in Table 3 for both z=1 and z=3. Overall, the clear trend is for the secondary BHs in small halos to be more strongly concentrated near the seed mass, while larger halos are more likely to have more massive secondary BHs. We emphasize that these trends are derived from the distributions for the mass ranges probed within the simulation, but are not reliable if used for masses

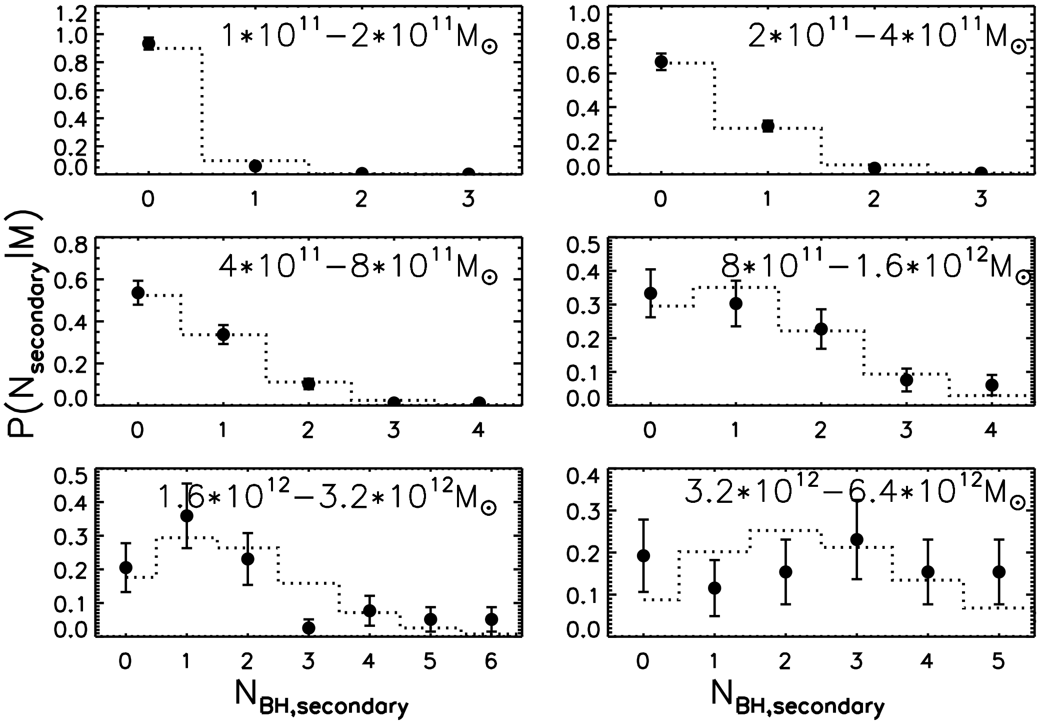

Figure 4. The probability distribution of $N_{\rm BH,secondary}$ for several host halo mass ranges. Filled circles show the results of our simulation (with Poisson error bars), and the dotted line shows a Poisson distribution centered about $\langle N_{\rm BH,secondary}\rangle$ for the given host halos.

Table 3. Fit for conditional mass function (Equations 4 and 5)

		Host Mass Range $\left(\log_{10}\left(\frac{M}{M_\odot}\right)\right)$			
		$11.5-12.5$	$12-13$	$12.5-13.5$	$13-14$
Primary BHs:					
z=1	μ	6.68	7.48	8.10	8.77
	σ	.48	.50	.42	.31
z=3	μ	6.54	7.28	8.30	N/A
	σ	.38	.75	.52	N/A
Secondary BHs:					
z=1	α	-1.51	-1.09	-1.01	-1.0
$\log_{10}\left(M_{0,\rm Host}\right)$		6.12	6.42	6.75	7.21
z=3	α	-1.79	-1.15	$-.71$	N/A
$\log_{10}\left(M_{0,\rm Host}\right)$		6.29	6.74	7.37	N/A

at or below the seed mass. We also note that μ is roughly proportional to the host mass, so the use of finite binsizes in $\log_{10}(M_{\rm host})$ increases σ above the ideal values for fixed halo masses.

3.3 Black Hole Radial Distribution

Another aspect of the HOD model is the spatial distribution of black holes within their parent halos. Although we have already analyzed how they populate subhalos within their hosts, it may also be useful to understand how BHs populate halos for which the subhalos have not been identified. For this, in Figure 6 we show the radial distribution of subhalos (dashed lines), BHs (solid lines), and secondary BHs (dotted lines) at redshift 1 for host groups separated into three mass bins (black: $10^{11}-10^{12}M_\odot$, blue: $10^{12}-10^{13}M_\odot$, green: $10^{13}-10^{14}M_\odot$), expressed as both a number density in units of R_{200}^{-3} (top), and simply as a number per radial bin (middle). In the lower plot we show the ratio of BHs to subhalos as a function of radial distance from the center. We do this using the complete BH population (left) and using only BHs above $10^7 M_\odot$ (right). Although only shown for $z=1$, we find very similar results for $z=3,5$ as well. Thus, although the number of BHs found in halos of a given mass changes with redshift (as seen in Table 2), the manner in which they are distributed within the halos remains approximately the same.

Figure 6 shows that for any host mass range, black holes are substantially more centrally-concentrated than the subhalos, as predicted by the black hole clustering properties in DeGraf et al. (2010b). In fact, they follow a fundamentally different profile which can be modeled by a simple power law rather than the more typical NFW profile (again in keeping with the results of DeGraf et al. 2010b). This increased concentration is a result of mergers between BH-hosting subgroups, typically between the central subgroup and a satellite. Because the central subgroup absorbs the satellite subgroup, the concentration of the subgroups does not increase, but that of the BHs will, since the BH will survive for a non-negligible time before a merging by the primary BH (and if it does, this is set by dynamical friction which is solved for in the simulations). Essentially, it is the existence of non-primary central BHs (see Figure 2) which

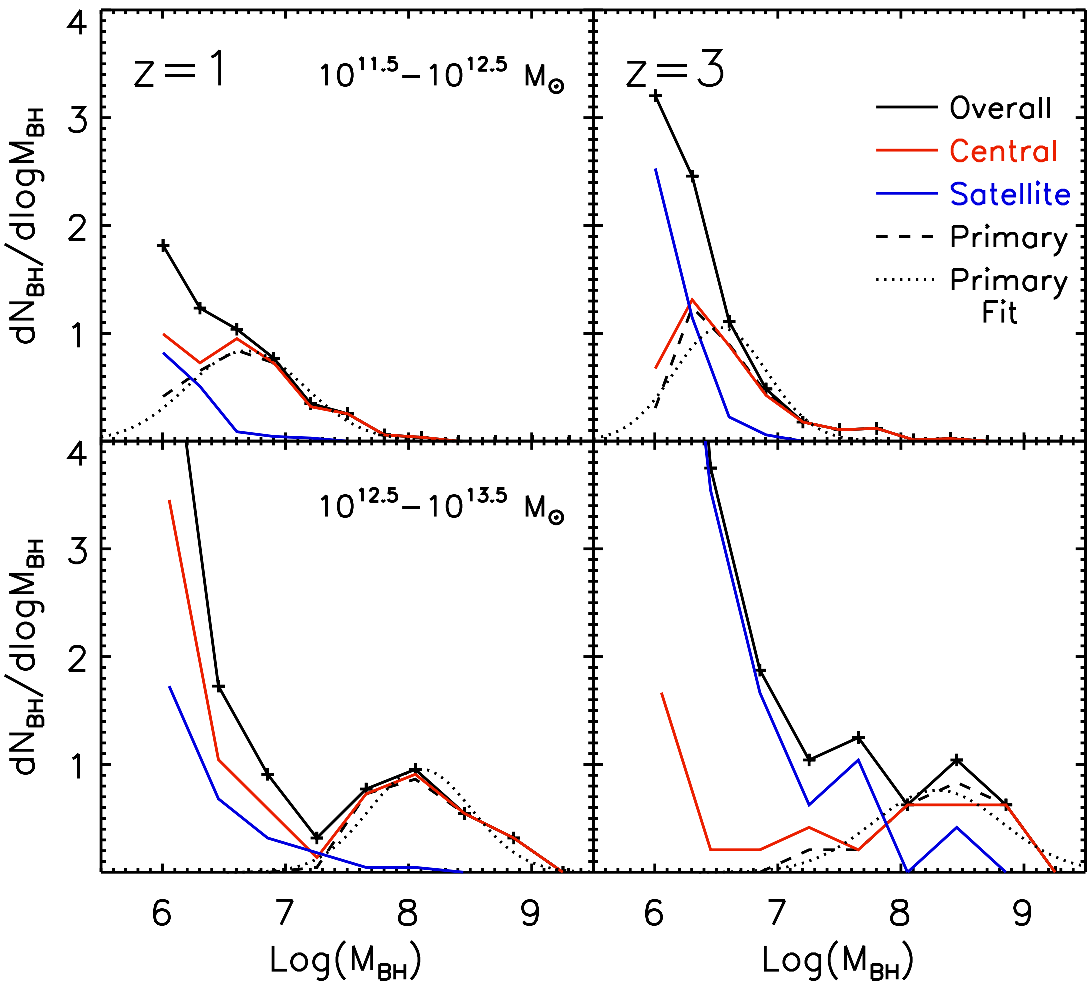

Figure 5. Distribution of BH masses in host halos of three different mass ranges at z=1 and 3. Note: Only a single group above $10^{13}M_\odot$ exists at z=3, so that distribution has not been plotted.

produces this increased central concentration. For further details see also DeGraf et al. (2010b).

To provide a means for modeling the spatial distribution of black holes within their parent halos (when populating halos directly rather than populating the central and satellite galaxies), we provide a simple fit to the radial profile (for $r < 2 \times r_{200}$) in form of a power law

$$n_{200}(r) \propto \left(\frac{r}{r_{200}}\right)^{\beta}, \tag{6}$$

which should be normalized to the occupation number found with Equation 1. The values for β are listed in Table 4. We note that for low-mass halos (below $\sim 10^{12}M_\odot$), the BHs are distributed roughly uniformly (in logarithmic bins) out to $\sim R_{200}$, while the most massive halos tend to have more BHs further from the center (though the density of BHs nonetheless decreases rapidly with radial distance). We also note that when approaching the group center, the ratio of BHs to subhalos tends to grow faster for low-mass halos than for more massive ones. Although this means that BHs in low mass halos are typically more centrally concentrated, we note that this is a result of the increased importance of the primary BH due to the smaller BH occupation number. However, we note that the ratio of secondary BHs to subhalos (dotted lines) is constant, regardless of host halo mass.

Table 4. Radial distribution parameter for functional form $n_{200}(r) \propto \left(\frac{r}{r_{200}}\right)^{\beta}$

Host Mass	β
$10^{11} - 10^{12}M_\odot$	-3.14
$10^{12} - 10^{13}M_\odot$	-2.89
$10^{13} - 10^{14}M_\odot$	-2.20

We also plot the radial distribution for massive BHs ($M_{\rm BH} > 10^7 M_\odot$, right column) in Figure 6. Here we see that in addition to being less common, the more massive BHs are more centrally concentrated than the less massive BHs. This is expected since the massive BHs are almost exclusively primary BH, and only rarely are they satelite BHs (see Figure 5), and thus they should be more highly concentrated toward the center of the group.

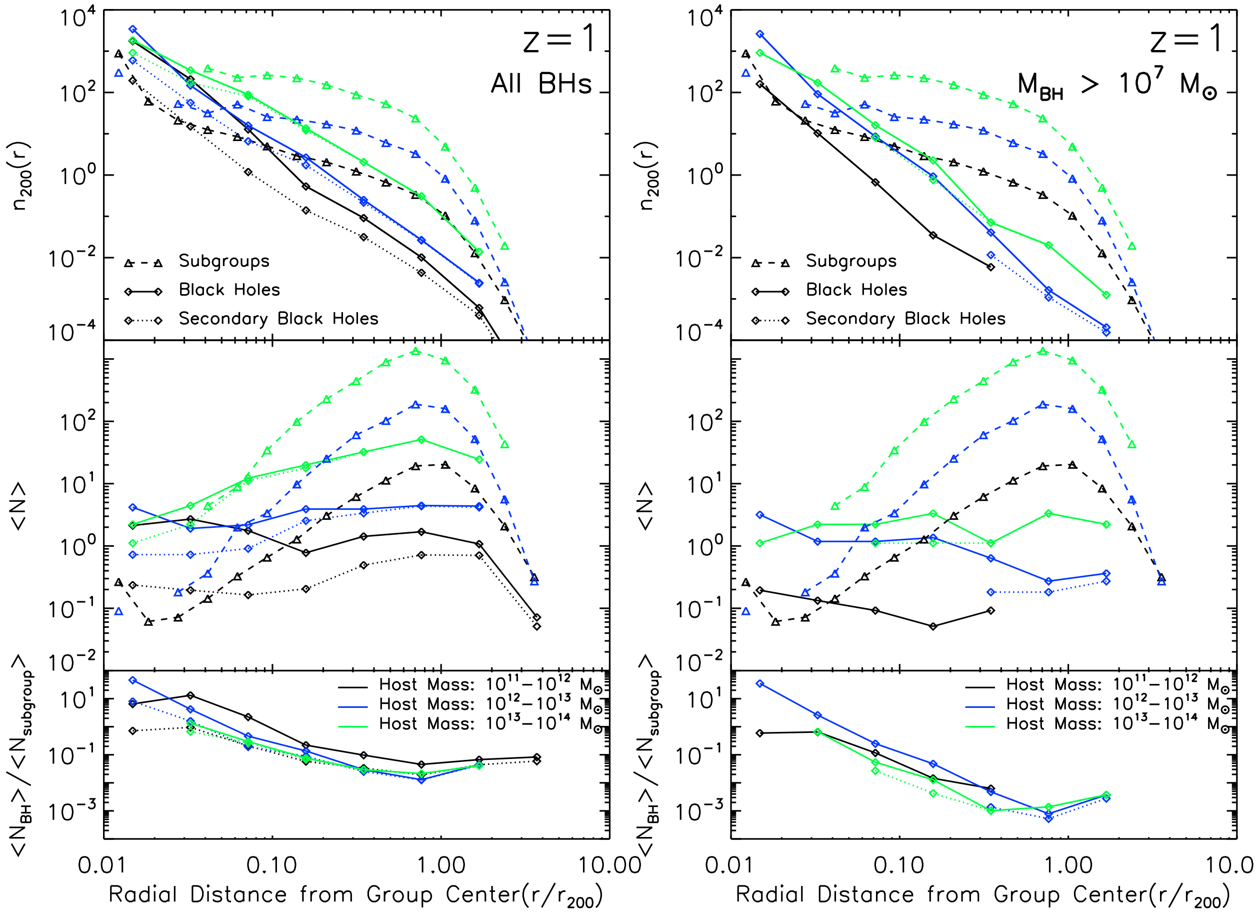

Figure 6. *Top:* Number density of subhalos (dashed lines), BHs (solid lines) and secondary BHs (dotted lines) in units of R_{200}^{-3} for all BHs (left) and for BHs above $10^7 M_\odot$ (right). *Middle:* Mean number of BHs (solid lines) and subhalos (dashed lines) per radial bin at z=1. *Bottom:* Ratio of BHs to subhalos as a function of radial distance from group center. In all plots, color represents the host group mass range (black - $10^{11} - 10^{12} M_\odot$; blue - $10^{12} - 10^{13} M_\odot$; green - $10^{13} - 10^{14} M_\odot$).

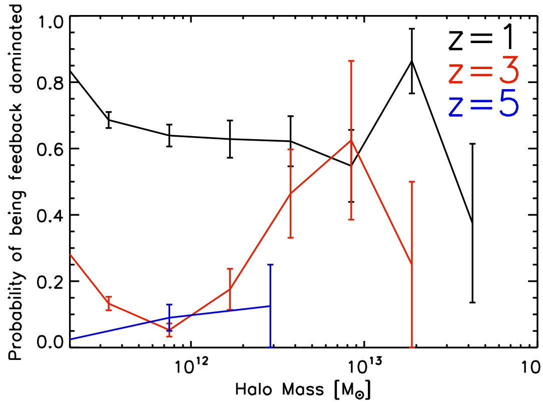

Figure 7. The fraction of groups which are feedback suppressed defined as $M_{\rm BH}$ above the quoted scatter of the $M - \sigma$ relation of Di Matteo et al. (2008) for z=1,3,5.

3.4 Black Hole Feedback Suppression

One final aspect of our analysis we would like to characterize is the mass of dark matter halos for which black hole feedback has been significant (and, for example, has been responsible for shutting down star formation in its halo.) In our model, and in others in the literature it has been shown that feedback from a central BH can create outflows that are able to expel a substantial amount of the gas from the host galaxy, thereby suppressing further growth of the BH, reproducing the $M - \sigma$ relation, and shutting down star formation (Di Matteo et al. 2005; Springel et al. 2005; Hopkins et al. 2006, 2007a; Di Matteo et al. 2008)

Here we fit our simulations to provide a probabilty for a given mass halo to have been significantly affected by BH feedback (i.e. feedback dominated). Di Matteo et al. (2008) showed that our model reprduced the observed $M - \sigma$ relation and it does so as a result of BH feedback. We use the $M - \sigma$ relation from our simulation to obtain the black hole mass and the respective halo mass for which BHs are feedback dominated.

In Figure 7 we show the fraction of groups in each halo mass bin whose BH is large enough to be considered 'feedback suppressed' (where the feedback is strong enough to suppress further growth), using the condition that any $M_{\rm BH}$ above the quoted scatter of the $M - \sigma$ relation of Di Matteo et al. (2008) is feedback suppressed. We note that the exact choice of cutoff threshold has a mild effect on the overall amplitude (i.e. the exact fraction of feedback suppressed halos), but the general trends are insensitive to the cutoff criteria. We find that at high redshift, very few halos have sufficiently large BHs to be feedback regulated, with larger halos being slightly more likely to have reached it than smaller halos. As time passes, the BHs in the high mass halos become more likely to become feedback regulated, and gradually the less-massive halos begin to become suppressed as well.

4 CONCLUSIONS

- The BH occupation number is well-described by the functional form $\langle N_{\rm BH}\rangle = 1 + \left(\frac{M}{M_0}\right)^{\alpha_{\rm tot}}$ for directly populating dark matter halos. Alternatively, separate occupation numbers can be obtained for BHs in central and satellite galaxies (Eqns. 2-3) to populate subgroups in an N-body simulation (or galaxy HOD model).
- In general, $\langle N_{\rm BH}\rangle$ typically follows $\langle N_{\rm subhalo}\rangle$ fairly consistently, suggesting BHs populate subhalos similarly regardless of host halo mass. At low redshift, however, we find there are fewer BHs in the hosts (both total and relative to $N_{\rm subhalo}$), particularly in moderate-mass halos, presumably as a result of the changing merger rates of both halos and the BHs within halos.
- The scatter in $\langle N_{\rm BH}\rangle$ is well described by a single primary BH and a number of secondary BHs that follow a Poisson distribution about the mean secondary occupation number $\langle N_{\rm BH,secondary}\rangle = \left(\frac{M_{\rm Host}}{M_0}\right)^{\alpha_{\rm tot}}$. We also find that the central and satellite occupation numbers follow approximate Poisson distributions.
- The conditional mass function for the primary BH peaks around a BH mass strongly correlated with $M_{\rm Host}$. The secondary BH mass distribution is peaked at the seed mass, and falls off as a power law in $M_{\rm BH}$. The power law is steepest for smaller host halos, such that more massive halos have a wider spread of BH masses, as expected.
- The spatial distribution of black holes within halos is fundamentally different from that of subhalos, tending to follow a power law rather than an NFW profile, leading to a significantly stronger central concentration of BHs relative to both subhalos and the underlying dark matter distribution. This increased concentration supports the predictions made in DeGraf et al. (2010b), though more direct investigation into our HOD-predicted correlation function will be investigated in an upcoming paper.
- For a given host halo mass, the spatial distribution of black holes does not evolve with redshift. Thus although the number of BHs per host halo changes with z, how they are distributed within these halos remains generally the same.
- At high redshift, few BHs are sufficiently massive to reach the observed $M-\sigma$ relation. When moving to lower redshifts, the more massive halos are generally the first to reach the $M-\sigma$ relation, with the lower-mass halos reaching the relation last. This suggests that the larger halos become suppressed by BH feedback at early time, and only at late times do the smaller halos begin to experience these suppressing effects of BH feedback.
- We have provided best fit parameters for the mean occupation number $\langle N_{\rm BH}\rangle$ as a function of host group mass, as well as the BH-mass and spatial distribution functions within these halos to provide the necessary information to populate dark matter halos with black holes. Alternatively, we have provided the mean occupation number of BHs found in the central and satellite galaxies ($\langle N_{\rm BH,cen}\rangle$ and $\langle N_{\rm BH,sat}\rangle$, respectively) to provide the necessary information for directly populating subgroups with BHs.

ACKNOWLEDGMENTS

We would like to thank Michael Busha for his suggestion to investigate when halos become black hole feedback dominated. This work was supported by the National Science Foundation, NSF Petapps, OCI-0749212 and NSF AST-0607819. The simulations were carried out at the NSF Teragrid Pittsburgh Supercomputing Center (PSC). D.N. was supported in part by the NSF grant AST-1009811, by NASA ATP grant NNX11AE07G, and by Yale University. Z.Z. gratefully acknowledges support from Yale Center for Astronomy and Astrophysics through a YCAA fellowship.

REFERENCES

Begelman M. C., Volonteri M., Rees M. J., 2006, MNRAS, 370, 289
Benson A. J., Cole S., Frenk C. S., Baugh C. M., Lacey C. G., 2000, MNRAS, 311, 793
Berlind A. A., Weinberg D. H., 2002, ApJ, 575, 587
Berlind A. A., et al., 2003, ApJ, 593, 1
Bondi H., 1952, MNRAS, 112, 195
Bondi H., Hoyle F., 1944, MNRAS, 104, 273
Bonoli S., Marulli F., Springel V., White S. D. M., Branchini E., Moscardini L., 2009, MNRAS, 606
Booth C. M., Schaye J., 2009, MNRAS, 398, 53
Bromm V., Larson R. B., 2004, ARA&A, 42, 79
Bromm V., Loeb A., 2003, ApJ, 596, 34
Brown M. J. I., et al., 2008, ApJ, 682, 937
Colberg J. M., di Matteo T., 2008, MNRAS, 387, 1163
Croft R. A. C., Di Matteo T., Springel V., Hernquist L., 2009, MNRAS, 400, 43
Croom S. M., et al., 2005, MNRAS, 356, 415
da Ângela J., et al., 2008, MNRAS, 383, 565
DeGraf C., Di Matteo T., Springel V., 2010a, MNRAS, 402, 1927
DeGraf C., Di Matteo T., Springel V., 2010b, ArXiv e-prints
Di Matteo T., Colberg J., Springel V., Hernquist L., Sijacki D., 2008, ApJ, 676, 33
Di Matteo T., Springel V., Hernquist L., 2005, Nature, 433, 604
Escala A., Larson R. B., Coppi P. S., Mardones D., 2004, ApJ, 607, 765
Ferrarese L., Merritt D., 2000, ApJL, 539, L9
Gebhardt K., et al., 2000, ApJL, 539, L13
Graham A. W., Driver S. P., 2007, ApJ, 655, 77
Haiman Z., Hui L., 2001, ApJ, 547, 27
Hennawi J. F., et al., 2006, AJ, 131, 1
Hopkins P. F., Hernquist L., Cox T. J., Di Matteo T., Robertson B., Springel V., 2006, ApJS, 163, 1
Hopkins P. F., Hernquist L., Cox T. J., Robertson B., Krause E., 2007a, ApJ, 669, 67

Hopkins P. F., Richards G. T., Hernquist L., 2007b, ApJ, 654, 731
Hoyle F., Lyttleton R. A., 1939, in Proceedings of the Cambridge Philosophical Society, vol. 35 of Proceedings of the Cambridge Philosophical Society, 405
Johansson P. H., Naab T., Burkert A., 2008, Astronomische Nachrichten, 329, 956
Kormendy J., Richstone D., 1995, ARA&A, 33, 581
Kravtsov A. V., Berlind A. A., Wechsler R. H., Klypin A. A., Gottlöber S., Allgood B., Primack J. R., 2004, ApJ, 609, 35
La Franca F., Andreani P., Cristiani S., 1998, ApJ, 497, 529
Lemson G., Kauffmann G., 1999, MNRAS, 302, 111
Lidz A., Hopkins P. F., Cox T. J., Hernquist L., Robertson B., 2006, ApJ, 641, 41
Magorrian J., et al., 1998, AJ, 115, 2285
Makino J., Funato Y., 2004, ApJ, 602, 93
Marconi A., Risaliti G., Gilli R., Hunt L. K., Maiolino R., Salvati M., 2004, MNRAS, 351, 169
Martini P., Weinberg D. H., 2001, ApJ, 547, 12
Mayer L., Kazantzidis S., Madau P., Colpi M., Quinn T., Wadsley J., 2007, Science, 316, 1874
Myers A. D., Brunner R. J., Nichol R. C., Richards G. T., Schneider D. P., Bahcall N. A., 2007a, ApJ, 658, 85
Myers A. D., Brunner R. J., Richards G. T., Nichol R. C., Schneider D. P., Bahcall N. A., 2007b, ApJ, 658, 99
Myers A. D., Richards G. T., Brunner R. J., Schneider D. P., Strand N. E., Hall P. B., Blomquist J. A., York D. G., 2008, ApJ, 678, 635
Porciani C., Magliocchetti M., Norberg P., 2004, MNRAS, 355, 1010
Reid B. A., Spergel D. N., 2009, ApJ, 698, 143
Robertson B., Hernquist L., Cox T. J., Di Matteo T., Hopkins P. F., Martini P., Springel V., 2006, ApJ, 641, 90
Ross N. P., et al., 2009, ApJ, 697, 1634
Seljak U., 2000, MNRAS, 318, 203
Shakura N. I., Sunyaev R. A., 1973, A&A, 24, 337
Shankar F., Salucci P., Granato G. L., De Zotti G., Danese L., 2004, MNRAS, 354, 1020
Shen Y., et al., 2007, AJ, 133, 2222
Shen Y., et al., 2009, ApJ, 697, 1656
Sijacki D., Springel V., di Matteo T., Hernquist L., 2007, MNRAS, 380, 877
Springel V., 2005, MNRAS, 364, 1105
Springel V., Di Matteo T., Hernquist L., 2005, MNRAS, 361, 776
Springel V., Hernquist L., 2003, MNRAS, 339, 289
Springel V., White S. D. M., Tormen G., Kauffmann G., 2001, MNRAS, 328, 726
Tremaine S., et al., 2002, ApJ, 574, 740
Volonteri M., Rees M. J., 2006, ApJ, 650, 669
Yang X., Mo H. J., van den Bosch F. C., 2003, MNRAS, 339, 1057
Yoshida N., Omukai K., Hernquist L., Abel T., 2006, ApJ, 652, 6
Yoshikawa K., Taruya A., Jing Y. P., Suto Y., 2001, ApJ, 558, 520
Zehavi I., et al., 2005, ApJ, 630, 1
Zehavi I., et al., 2010, ArXiv e-prints
Zheng Z., 2004, ApJ, 610, 61
Zheng Z., et al., 2005, ApJ, 633, 791
Zheng Z., Coil A. L., Zehavi I., 2007, ApJ, 667, 760